Amnesia Following Herpes Simplex Encephalitis: Diffusion-Tensor Imaging Uncovers Reduced Integrity of Normal-appearing White Matter[1]

Håkon Grydeland, Cand Psychol
Kristine B. Walhovd, PhD
Lars T. Westlye, Cand Psychol
Paulina Due-Tønnessen, MD
Vidar Ormaasen, PhD
Øyvind Sundseth, Cand Psychol
Anders M. Fjell, PhD

Purpose: To explore white matter (WM) and gray matter tissue integrity in the apparently unaffected hemisphere of patients with herpes simplex encephalitis (HSE) who have gross unilateral medial temporal lobe (MTL) lesions and both verbal and visuospatial memory deficits.

Materials and Methods: This study had institutional ethics committee approval and included written informed consent. Magnetic resonance (MR) imaging was performed in five patients who had recovered from HSE (one woman, four men; median age, 32 years; interquartile range, 28.5–37 years) and 51 age-matched controls (30 women, 21 men; median age, 32 years; interquartile range, 28–37 years). As markers of microstructural WM integrity, fractional anisotropy (FA), mean diffusivity (MD), axial diffusivity, and radial diffusivity (RD) derived from diffusion-tensor (DT) imaging were used. An automated regional brain segmentation approach yielded estimates of subcortical volumes, including hippocampus, and cortical thickness. Group differences were evaluated by using permutation tests.

Results: Examination of standard MR images found unilateral lesions in all patients. The patients with HSE showed reduced FA and increased MD and RD in several WM tracts contralateral to lesions ($P < .05$, corrected for multiple comparisons). Affected tracts included connections between the MTLs and other parts of the brain. No significant group differences were observed in subcortical volume or cortical thickness.

Conclusion: These results suggest that patients with HSE have reduced microstructural integrity of normal-appearing WM contralateral to grossly visible lesions. These subtle lesions, detectable at DT imaging, probably contribute to the memory impairment manifested by these patients.

Supplemental material: *http://radiology.rsna.org/lookup/suppl/doi:10.1148/radiol.10100179/-/DC1*

[1] From the Center for the Study of Human Cognition, Department of Psychology, University of Oslo, PO Box 1094, Blindern, 0317 Oslo, Norway (H.G., K.B.W., L.T.W., A.M.F.); Departments of Neuropsychology (Ø.S., K.B.W., A.M.F.) and Infectious Diseases (V.O.), Ullevaal University Hospital, Oslo, Norway; and Department of Radiology, Rikshospitalet University Hospital, Oslo, Norway (P.D.). Received January 25, 2010; revision requested March 17; revision received May 14; accepted May 27; final version accepted July 7. Supported by the Norwegian Research Council (H.G., student research fellowship; K.B.W., grants 186092 and 177404). **Address correspondence to** H.G. (e-mail: *hakon.grydeland@psykologi.uio.no*).

Herpes simplex encephalitis (HSE) may cause gross uni- or bilateral cerebral lesions, usually affecting the medial temporal lobes (MTLs) (ie, hippocampal formation, entorhinal and parahippocampal areas), that are readily imaged by using standard spin-echo magnetic resonance (MR) sequences (1,2). As all cellular elements are affected, lesions may comprise both white matter (WM) and gray matter (3). Cognitively, the most common long-term sequela in HSE is anterograde amnesia (4): the impaired ability to form new episodic memories.

Anterograde amnesia involving both verbal and visuospatial memory has previously been indicated in patients with HSE who have unilateral temporal lesions (2,5). Researchers in other previous studies (6,7) have reported that damage to the dominant MTL (usually the left) impairs verbal memory, while damage to the nondominant MTL (usually the right) impairs visuospatial memory. Follow-up analyses of patients who have undergone unilateral temporal lobectomy and have anterograde amnesia have shown hitherto undiscovered contralateral MTL damage (8). Thus, patients with HSE who have both verbal and visuospatial amnesia may have lesions in normal-appearing brain tissue contralateral to the primary lesion, even when such lesions are not detectable with standard MR imaging pulse sequences.

Diffusion-tensor (DT) imaging offers a noninvasive method to explore WM integrity in vivo. Deviations in diffusion characteristics may be detected in normal-appearing WM, indicating abnormalities that are not visible on standard T1- or T2-weighted MR images (9). We hypothesized that patients with HSE would show less anisotropic diffusion, smaller subcortical volumes, and thinner cortices in the MTL of the apparently unaffected hemisphere compared with healthy age-matched controls. The purpose of our study was to explore WM and gray matter tissue integrity in the apparently unaffected hemisphere of patients with HSE who have gross unilateral MTL lesions and both verbal and visuospatial memory deficits.

Advances in Knowledge

- Reduced microstructural integrity of normal-appearing white matter (WM) was observed contralateral to gross unilateral lesions following herpes simplex encephalitis (HSE).
- The subtle lesions in normal-appearing WM were not evident at conventional MR imaging but could be detected at diffusion-tensor (DT) imaging analysis.
- The severe amnesia of patients with HSE, usually related to bilateral lesions, is likely caused in part by the reduced WM integrity in tracts connecting the medial temporal lobe to other parts of the brain in the apparently unaffected hemisphere.

Implications for Patient Care

- Subtle lesions following HSE can be identified at DT imaging analysis in areas that appear normal with other imaging techniques, implying that DT imaging–derived measures are useful in diagnosis and prognosis.
- The lesions in normal-appearing WM likely contribute to the memory impairments typically experienced by patients with HSE, and knowledge of such functional effects may facilitate rehabilitation.

Materials and Methods

Subjects

Our study was approved by the institutional ethics committee, and all retrospectively enrolled participants gave written informed consent.

We identified nine patients with HSE who fulfilled the inclusion criterion of lesions affecting the MTL. Patients were required not to be using medicines that affect the central nervous system and not to have secondary injuries, diseases, or complications related to HSE. We excluded one patient owing to prolonged respirator treatment during hospitalization, and three patients declined to participate. The final sample consisted of five patients who had recovered from HSE (one woman, four men; median age, 32 years; interquartile range [IQR], 28.5–37 years), all of whom had positive polymerase chain reaction findings for herpes simplex virus type 1. Median time since the insult was 4 years (IQR, 2–7 years). One patient was left-handed.

A neuroradiologist (P.D., with 21 years experience) examined all MR images. In all patients, liquefied cavities were observed in the MTL, with signal changes in adjacent tissue (Fig 1). Lesions were deemed unilateral, involving the left (n = 3) or right (n = 2) hemisphere. The term *contralateral hemisphere* in the following text indicates the hemisphere contralateral to the HSE lesion.

The control group included 51 age-matched healthy volunteers (30 women, 21 men; median age, 32 years; IQR, 28–37 years) drawn from a sample described in detail elsewhere (10). Appendix E1 (online) and Table E1

Published online before print
10.1148/radiol.10100179

Radiology 2010; 257:774–781

Abbreviations:
AD = axial diffusivity
DT = diffusion tensor
FA = fractional anisotropy
HSE = herpes simplex encephalitis
HSE_L = HSE lesion in left hemisphere
HSE_R = HSE lesion in right hemisphere
IQR = interquartile range
MD = mean diffusivity
MTL = medial temporal lobe
RD = radial diffusivity
WM = white matter

Author contributions
Guarantor of integrity of entire study, H.G.; study concepts/study design or data acquisition or data analysis/interpretation, all authors; manuscript drafting or manuscript revision for important intellectual content, all authors; approval of final version of submitted manuscript, all authors; literature research, H.G., L.T.W., P.D., V.O.; clinical studies, L.T.W., P.D., Ø.S., A.M.F.; statistical analysis, H.G., L.T.W., A.M.F.; and manuscript editing, H.G., K.B.W., L.T.W., P.D., V.O., A.M.F.

Authors stated no financial relationship to disclose.

Figure 1

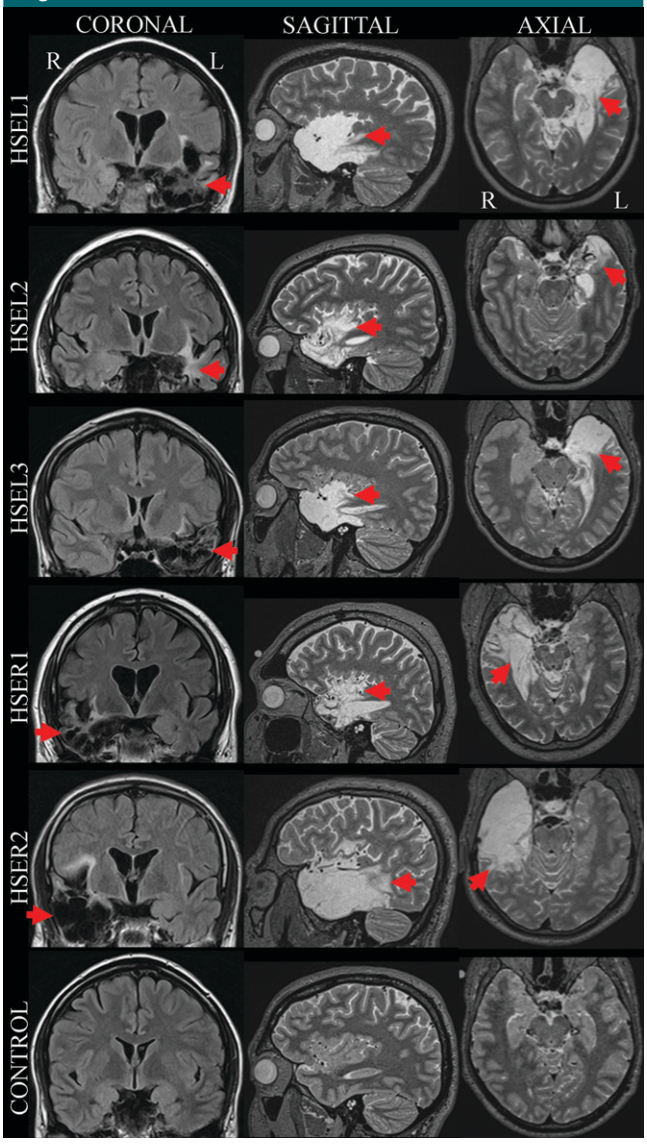

Figure 1: Unenhanced coronal fluid-attenuated inversion-recovery, or FLAIR, (repetition time msec/echo time msec, 9000/109) and sagittal and axial sampling perfection with application-optimized contrasts by using different flip angle evolutions, or SPACE, (3390/388) T2-weighted structural MR images of five HSE patients and one control (32-year-old man). Arrows = lesions, *HSEL* = HSE lesion in left hemisphere (HSE_L), *HSER* = HSE lesion in right hemisphere (HSE_R), *L* = left, *R* = right.

(online) summarize sample characteristics and results of the neuropsychologic assessment.

MR Imaging Acquisition

Imaging data were acquired by using a 12-channel head coil with a 1.5-T MR imager (Avanto; Siemens Medical Solutions, Erlangen, Germany). MR examinations included two T2-weighted pulse sequences: fluid-attenuated inversion-recovery repetition time (repetition time msec/echo time msec/inversion time msec, 9000/109/2500; matrix, 448 × 512; field of view, 448; voxel size, 0.45 × 0.45 × 6.50 mm), or FLAIR, and sampling perfection with application-optimized contrasts by using different flip angle evolutions (3390/388; matrix, 204 × 256; field of view, 204; isotropic voxels, 1 mm), or SPACE.

The DT imaging was performed with a single-shot twice-refocused spin-echo echo-planar sequence (8200/82; *b* value, 700 sec/mm^2; isotropic voxels, 2 mm). The sequence was repeated in two runs of 30 gradient directions. Ten images with a *b* value of 0 sec/mm^2 (hereafter, b_0 image or volume) were obtained per run. For morphometry, we used a repeated T1-weighted magnetization-prepared rapid gradient-echo sequence (2400/3.61/1000; matrix, 192 × 192; field of view, 240; voxel size, 1.25 × 1.25 × 1.20 mm). DT and magnetization-prepared rapid gradient-echo acquisitions were averaged during postprocessing to increase the signal-to-noise ratio.

DT Imaging Analysis

Data were analyzed by using FSL software tools (FMRIB Software Library, available at *http://www.fmrib.ox.ac.uk/fsl*) (H.G. and L.T.W., with 2 and 5 years experience, respectively). Each volume was affine registered to the b_0 volume by using FLIRT (FMRIB Software Library) and correcting for motion between acquisitions and eddy currents. After removing nonbrain tissue, fractional anisotropy (FA) and eigenvalue maps were computed. We defined mean diffusivity (MD) as the mean of the three eigenvalues, axial diffusivity (AD) as the largest eigenvalue, and radial diffusivity (RD) as the mean of the second and third eigenvalues. (The nomenclature *axial* and *radial* diffusivity pertains to the eigenvalues of the DT relative to the principal eigenvector and not necessarily to the underlying brain tissue.) FA volumes were skeletonized and transformed into a common space by using tract-based spatial statistics (11). The tract-based spatial statistics steps were executed separately for the HSE_L and control groups and for the HSE_R and control groups. All volumes were nonlinearly warped to the FMRIB58_FA template by using FNIRT (FMRIB Software Library). Inaccurate warping may occur when structures are present in

the standard, but not native, brain, and to account for this, areas showing signal intensity changes in the b_0 volumes were masked. Thus, the warping was based only on structures present in both native and standard spaces, and accuracy was judged to be satisfactory (H.G. and L.T.W.).

Mean FA volume across subjects was computed and thinned to generate a mean FA skeleton. We set a threshold for the skeleton at an FA greater than 0.20 to minimize partial voluming and excluded parts of the skeleton that intersected the gross lesions. Individual FA values were projected onto the skeleton, and the resulting data were fed into voxelwise statistics. Similar analyses were used for MD, AD, and RD.

To verify that significant effects were not due to errors in registration procedures or other processing steps, we *(a)* back-projected significant FA effects to each participant's native diffusion space and *(b)* obtained FA, MD, and RD directly from a temporal lobe region of interest in native diffusion space and tested for group differences (H.G.).

Morphometric Analyses

Regional subcortical volumes and cortical thickness were obtained by using FreeSurfer software tools (Athinoula A. Martinos Center for Biomedical Imaging, available at *http://surfer.nmr.mgh.harvard.edu*). For volume calculations of subcortical structures, we used whole-brain segmentation, which has been described in detail elsewhere (12). Cortical thickness measurements were obtained by reconstructing representations of the boundary between WM and gray matter and the cortical surface and calculating the distance between these surfaces at each vertex across the mantle (13). Maps were smoothed with a full width at a half maximum of 30 mm and averaged across participants. We visually checked all segmentations in the contralateral hemisphere for accuracy and corrected minor errors, usually restricted to removal of nonbrain tissue included in the cortical surface (H.G. and L.T.W.). Intracranial volume was estimated by using an atlas-based normalization procedure implemented in FreeSurfer.

Statistical Analyses

Voxelwise DT imaging analyses for group effects (ie, HSE_L group vs controls, HSE_R group vs controls) on FA, MD, AD, and RD were performed by using permutation-based nonparametric cluster inference as implemented in Randomise (FMRIB Software Library), which is a permutation program. Threshold-free cluster enhancement was used for statistical inference (14). For the HSE_L group versus controls, 10000 permutations were performed. Owing to the smaller sample size, 1378 permutations were performed for the HSE_R group versus controls.

To test for group effects on regional subcortical volumes while controlling for intracranial volume, we first performed linear regression analyses with each volume as the dependent variable and intracrainal volume as the independent variable, saving the unstandardized residuals. These residuals were then fed into permutation tests by using custom Matlab (Mathworks, Nattick, Mass) scripts to test for median differences between groups. *P* values were Bonferroni corrected by a factor of 46. Vertexwise analyses for group effects on cortical thickness were carried out with cluster sizes tested nonparametrically against empirical null distributions as above. For all measures, we only considered effects in the contralateral hemisphere. *P* values less than .05 were considered to indicate significant differences. Group differences in neuropsychologic measures were evaluated by using the Mann-Whitney test.

Results

MR images obtained with standard sequences showed unilateral lesions in all patients.

Behavioral Results

There were no significant differences between patients and controls in 12 of the 16 sample characteristics and neuropsychologic assessment measures, including age and performance intelligence quotient. Significant group differences were observed in education (patients < controls), Stroop interference (patients > controls), verbal fluency categories (patients < controls), and verbal intelligence quotient (patients < controls) (Appendix E1 [online]).

Patients performed significantly worse on both verbal and visuospatial memory tests, including all subtests of the California Verbal Learning Test (CVLT) and Rey-Osterrieth Complex Figure Test (ROCF) delayed recall (5 and 30 minutes) (all $P < .01$). For instance, patients with HSE scored a median of 22 on the CVLT learning subtest and a median of 1 on the CVLT 5-minute delayed recall subtest, compared with 60 and 14, respectively, for the controls (Table E2 [online]). Continuous Visual Memory Test (CVMT) delayed recognition scores tended to be lower for patients ($P = .0504$), while scores on CVMT total and the initial ROCF copy did not show any significant group differences.

DT Imaging Analyses

Figure 2 depicts voxels showing reduced FA and increased MD and RD in the patients compared with the controls ($P < .05$, corrected for multiple comparisons). The Table gives a summary of the regional effects (corresponding FA, MD, and RD values are presented in Table E3 [online]). Median FA in the areas showing significant group differences in the contralateral hemisphere was 0.47 (IQR, 0.47–0.54) for the HSE_L group and 0.57 (IQR, 0.55–0.59) for controls, a 19% difference. It was 0.43 (IQR, 0.43–0.44) for the HSE_R group and 0.51 (IQR, 0.50–0.53) for controls, a 17% difference. No areas showed increased FA in the patients.

Median MD in areas showing significant group differences in the contralateral hemisphere was 0.85×10^{-3} mm^2/sec (IQR, [0.74–0.90] $\times 10^{-3}$ mm^2/sec) for the HSE_L group and 0.72×10^{-3} mm^2/sec (IQR, [0.69–0.75] $\times 10^{-3}$ mm^2/sec) for controls, a difference of 17%. It was 0.89×10^{-3} mm^2/sec (IQR, [0.88–0.90] $\times 10^{-3}$ mm^2/sec) for the HSE_R group and 0.79×10^{-3} mm^2/sec (IQR, [0.76–0.82] $\times 10^{-3}$ mm^2/sec) for

Figure 2

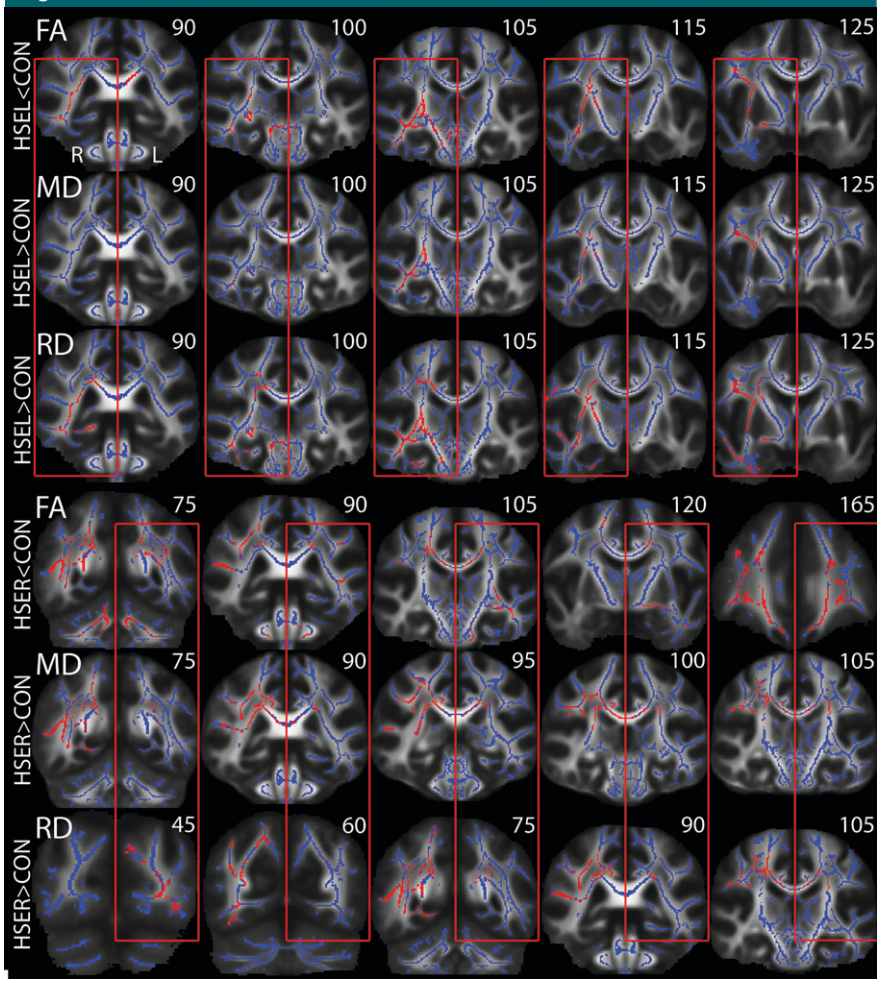

Figure 2: Mean tract-based spatial statistics skeletons (blue) superimposed on the mean FA images show voxelwise group differences (red voxels; $P < .05$, corrected for multiple comparisions) for FA, MD, and RD. Top three rows: HSE_L *(HSEL)* group versus controls *(CON)* (tract-based spatial statistics skeleton mask = 122 373 WM voxels). Bottom three rows: HSE_R *(HSER)* group versus controls (tract-based spatial statistics skeleton mask = 118 710 WM voxels). Both patient groups showed reduced FA and increased MD and RD in the contralateral hemisphere (red boxes) compared with controls. Number in upper right corner of each image is the Montreal Neurological Institute *y* coordinate.

controls, a difference of 12%. No areas showed decreased MD in the patients.

Median RD in areas showing significant group differences in the contralateral hemisphere was 0.63×10^{-3} mm^2/sec (IQR, $[0.52–0.64] \times 10^{-3}$ mm^2/sec) for the HSE_L group and 0.50×10^{-3} mm^2/sec (IQR, $[0.47–0.53] \times 10^{-3}$ mm^2/sec) for controls, a 23% difference. It was 0.63×10^{-3} mm^2/sec (IQR, $[0.62–0.65] \times 10^{-3}$ mm^2/sec) for the HSE_R group and 0.54×10^{-3} mm^2/sec (IQR, $[0.52–0.56] \times 10^{-3}$ mm^2/sec) for controls, a 15% difference. No areas showed decreased RD in the patients.

No significant differences were found in AD between patients and controls in the contralateral hemisphere.

Figure E2 (online) shows back-projected significant FA effects superimposed on the FA volumes of each patient and five age- and gender-matched controls, demonstrating good alignment between the skeleton and the native space in the temporal areas. In addition, FA, MD, and RD values obtained directly from the temporal lobe region of interest in diffusion space also differed significantly between groups, further verifying that the observed effects were not due to registration or other processing errors (Table E4 [online], Fig E3 [online]).

Morphometric Analyses

No significant differences between patients and controls were observed in subcortical volumes (including hippocampus) or cortical thickness in the contralateral hemisphere (Fig E4 [online]).

Discussion

In our study, memory-impaired HSE patients with unilateral lesions on standard MR images were shown to have areas of altered diffusivity in the hemisphere contralateral to the MR-detected lesions. Notably, these contralateral abnormalities in diffusivity affected tracts connecting the MTL with other parts of the brain, including those involved in memory processing (15). Researchers in previous studies of HSE have reported changes in WM diffusivity (16,17) and volume (18,19) in temporal areas comprising these tracts. However, these studies did not explore normal-appearing brain tissue specifically. Our findings suggest that reduced WM integrity in seemingly unaffected areas in the hemisphere contralateral to the primary HSE lesions is involved in the impaired memory observed in these patients.

The reduced WM integrity could be explained by bilateral damage caused directly by the herpes simplex virus or by secondary immune-mediated mechanisms (20). Postmortem findings in 29 patients with HSE invariably showed bilateral asymmetric distribution of herpes simplex virus antigen in different brain areas (including MTL), indicative of disease progression from one hemisphere to the other (21). Acyclovir treatment may hamper this bilateral spread (22), but both hemispheres could still be affected even if it is not observable at neuroradiologic examination. It has been published (1) that MR spectroscopy of one patient with HSE who had only right temporal lobe

Number of Voxels Showing Significant Differences in FA, MD, and RD in Patient Groups versus Controls

	HSE_L Group			HSE_R Group		
Tract	FA	MD	RD	FA	MD	RD
Anterior corona radiata	NS	NS	156 (10)	1054 (63)	NS	NS
Anterior thalamic radiation	259 (4)	7 (0)	282 (5)	1253 (17)	143 (2)	133 (2)
Cerebellar peduncle	11 (1)	NS	22 (1)	686 (37)	NS	NS
Corpus callosum						
Body	NS	NS	90 (6)	494 (31)	199 (12)	193 (12)
Splenium	NS	NS	228 (19)	139 (12)	86 (7)	99 (8)
Corticospinal	777 (17)	225 (5)	1063 (23)	471 (11)	144 (3)	115 (3)
Dorsal cingulum	NS	NS	NS	580 (27)	1 (0)	77 (4)
External capsule	519 (41)	294 (23)	536 (42)	90 (6)	NS	NS
Forceps major	NS	NS	22 (1)	50 (2)	13 (0)	280 (10)
Fornix and stria terminalis	154 (59)	31 (12)	119 (45)	87 (26)	NS	NS
Inferior fronto-occipitial fasciculus	1171 (13)	368 (4)	1240 (14)	1589 (19)	40 (0)	294 (4)
Inferior longitudinal fasciculus	800 (13)	302 (5)	1282 (21)	714 (10)	61 (1)	267 (4)
Internal capsule						
Posterior limb	369 (41)	155 (17)	432 (48)	NS	NS	NS
Retrolenticular part	433 (57)	57 (7)	365 (48)	79 (11)	NS	NS
Parahippocampal cingulum	NS	NS	246 (35)	NS	NS	7 (1)
Posterior corona radiata	36 (5)	NS	120 (16)	126 (18)	212 (30)	193 (28)
Superior corona radiata	198 (14)	119 (8)	621 (44)	246 (18)	68 (5)	120 (9)
Superior longitudinal fasciculus						
Entire tract	585 (8)	538 (7)	1086 (15)	851 (11)	7 (0)	3 (0)
Temporal part	417 (14)	257 (9)	562 (19)	448 (10)	NS	NS
Unicinate fasciculus	39 (2)	NS	100 (4)	970 (27)	NS	NS

Note.—Data are numbers of voxels significantly different from those in controls, with percentage of total voxels in that tract in parentheses. Changes in HSE_L group were in the right hemisphere, and those in the HSE_R group were in the left hemisphere. Binary masks based on probabilistic Johns Hopkins University WM tractography atlas and on the International Consortium for Brain Mapping DTI-81 WM labels atlas indicated the anatomic localization (14) (see Figure E1 [online] for tract renderings). NS = no significant differences.

damage visible on T1- and T2-weighted MR images showed a reduced *N*-acetylaspartate–to-choline ratio, indicating neuronal loss, in the normal-appearing left temporal lobe. On the basis of our current data, we cannot rule out the possibility that the altered diffusivity is mediated by secondary lesion-related mechanisms (9). Images from acute stages are needed to address the question of direct and secondary effects. The RD increases observed in our study may partly be caused by demyelination (23,24), although other factors, such as axonal loss, fiber density, axonal diameter, and integrity of cell membranes, probably contribute considerably to the degree of anisotropy (25).

No group differences in subcortical volumes (including hippocampus) or cortical thickness were observed in the contralateral hemisphere after multiple-comparisons correction. Subcortical volume and cortical thickness reductions in the MTL have been documented in HSE (18,19,26), but not specifically concerning normal-appearing brain tissue. In 35 patients with primary progressive multiple sclerosis who had reduced FA in normal-appearing WM tracts, Bodini et al (27) found gray matter atrophy in some anatomically corresponding areas but not others. DT imaging and morphometry may therefore be complementary and relatively independent neurobiologic markers of subtle structural alterations (28). Accordingly, we have previously found that DT imaging indexes are sensitive to normal age-related WM changes decades prior to tissue loss (10). Thus, subtle pathologic changes may manifest primarily as microstructural changes as measured at DT imaging and, to a lesser extent, in morphology, at least in some areas. However, the limited statistical power of our study may have precluded detection of subtle morphometric effects, and it is premature to conclude that such effects do not exist on the basis of our analyses. Larger samples are needed to explore this hypothesis.

Diffusion properties of the arcuate fasiculus, fornix, inferior fronto-occipital fasciculus, inferior longitudinal fasciculus, parahippocampal cingulum, and uncinate fasciculus have been related to memory functions in epilepsy and schizophrenia (29,30). In our study, differences in diffusivity between patients and controls were observed in all these tracts. Patients also showed substantial deficits on tests assessing verbal and visuospatial memory. Researchers in previous lesion (6,7) and functional MR imaging (31,32) studies have reported

material-specific lateralization of verbal and visuospatial memory function; bilateral damage could thus be necessary to cause memory impairment in both domains. Consequently, one may infer that the altered diffusivity in the contralateral hemisphere contributed to the memory deficits in these patients with HSE.

Inferences about functional memory effects should be drawn with caution. Reports of memory deficits for verbal (32,33) and visuospatial (34) material following both left and right unilateral lesions suggest that unilateral lesions may be sufficient to cause both verbal and visuospatial memory impairment. However, these previous findings do not mean that bilateral damage will not cause further memory problems. Rather, both verbal and visuospatial memory may be dependent on the integrity of both the left and right MTLs (34). This hypothesis is supported by a functional imaging study that showed bilateral MTL activity with verbal material (32). Thus, altered diffusivity in tracts connecting the MTLs to other brain areas likely contributes to the severe memory deficits in patients with HSE.

A major limitation of our study was the small patient sample. The rare occurrence of HSE, estimated at an annual incidence between two and three cases per million people (35), limits the recruitment of large groups, as indicated by other morphometric studies that have used a similar number of HSE participants (18,26). However, the small patient sample reduced statistical power, and further studies, preferably with larger samples, are required to confirm our findings.

Future studies should further examine the functional effects of the changes seen at DT imaging and may profit from a longitudinal design, particularly including imaging during acute phases, to allow for clearer inferences about neurobiologic mechanisms. Inclusion of patients with HSE who have a degree of tissue affection that is similar to that which we described here but who have no evidence of cognitive deficits, if such patients indeed exist, would be particularly beneficial for inferences of structure-function relationships.

References

1. Demaerel P, Wilms G, Robberecht W, et al. MRI of herpes simplex encephalitis. Neuroradiology 1992;34(6):490–493.
2. Kapur N, Barker S, Burrows EH, et al. Herpes simplex encephalitis: long term magnetic resonance imaging and neuropsychological profile. J Neurol Neurosurg Psychiatry 1994; 57(11):1334–1342.
3. Baringer JR. Herpes simplex infections of the nervous system. Neurol Clin 2008;26(3): 657–674, viii.
4. Hokkanen L, Launes J. Neuropsychological sequelae of acute-onset sporadic viral encephalitis. Neuropsychol Rehabil 2007;17(4-5): 450–477.
5. Utley TF, Ogden JA, Gibb A, McGrath N, Anderson NE. The long-term neuropsychological outcome of herpes simplex encephalitis in a series of unselected survivors. Neuropsychiatry Neuropsychol Behav Neurol 1997;10(3):180–189.
6. Frisk V, Milner B. The role of the left hippocampal region in the acquisition and retention of story content. Neuropsychologia 1990; 28(4):349–359.
7. Smith ML, Milner B. The role of the right hippocampus in the recall of spatial location. Neuropsychologia 1981;19(6):781–793.
8. Baxendale S. Amnesia in temporal lobectomy patients: historical perspective and review. Seizure 1998;7(1):15–24.
9. Werring DJ, Clark CA, Barker GJ, Thompson AJ, Miller DH. Diffusion tensor imaging of lesions and normal-appearing white matter in multiple sclerosis. Neurology 1999;52(8): 1626–1632.
10. Westlye LT, Walhovd KB, Dale AM, et al. Life-span changes of the human brain white matter: diffusion tensor imaging (DTI) and volumetry. Cereb Cortex 2010;20:2055–2068.
11. Smith SM, Jenkinson M, Johansen-Berg H, et al. Tract-based spatial statistics: voxelwise analysis of multi-subject diffusion data. Neuroimage 2006;31(4):1487–1505.
12. Fischl B, Salat DH, Busa E, et al. Whole brain segmentation: automated labeling of neuroanatomical structures in the human brain. Neuron 2002;33(3):341–355.
13. Fischl B, Dale AM. Measuring the thickness of the human cerebral cortex from magnetic resonance images. Proc Natl Acad Sci U S A 2000;97(20):11050–11055.
14. Smith SM, Nichols TE. Threshold-free cluster enhancement: addressing problems of smoothing, threshold dependence and localisation in cluster inference. Neuroimage 2009;44(1):83–98.
15. Mori S, Wakana S, van Zijl PCM, Nagae-Poetscher LM. MRI atlas of human white matter. Amsterdam, the Netherlands: Elsevier, 2005.
16. Herweh C, Jayachandra MR, Hartmann M, et al. Quantitative diffusion tensor imaging in herpes simplex virus encephalitis. J Neurovirol 2007;13(5):426–432.
17. Sener RN. Herpes simplex encephalitis: diffusion MR imaging findings. Comput Med Imaging Graph 2001;25(5):391–397.
18. Noppeney U, Patterson K, Tyler LK, et al. Temporal lobe lesions and semantic impairment: a comparison of herpes simplex virus encephalitis and semantic dementia. Brain 2007;130(pt 4):1138–1147.
19. Yoneda Y, Mori E, Yamashita H, Yamadori A. MRI volumetry of medial temporal lobe structures in amnesia following herpes simplex encephalitis. Eur Neurol 1994;34(5): 243–252.
20. Meyding-Lamadé U, Lamadé W, Kehm R, et al. Herpes simplex virus encephalitis: chronic progressive cerebral MRI changes despite good clinical recovery and low viral load—an experimental mouse study. Eur J Neurol 1999;6(5):531–538.
21. Esiri MM. Herpes simplex encephalitis: an immunohistological study of the distribution of viral antigen within the brain. J Neurol Sci 1982;54(2):209–226.
22. Meyding-Lamadé UK, Oberlinner C, Rau PR, et al. Experimental herpes simplex virus encephalitis: a combination therapy of acyclovir and glucocorticoids reduces long-term magnetic resonance imaging abnormalities. J Neurovirol 2003;9(1):118–125.
23. Song SK, Sun SW, Ramsbottom MJ, Chang C, Russell J, Cross AH. Dysmyelination revealed through MRI as increased radial (but unchanged axial) diffusion of water. Neuroimage 2002;17(3):1429–1436.
24. Koenig H, Rabinowitz SG, Day E, Miller V. Post-infectious encephalomyelitis after successful treatment of herpes simplex encephalitis with adenine arabinoside: ultrastructural observations. N Engl J Med 1979;300(19): 1089–1093.
25. Beaulieu C. The basis of anisotropic water diffusion in the nervous system: a technical review. NMR Biomed 2002;15(7-8): 435–455.
26. Gitelman DR, Ashburner J, Friston KJ, Tyler LK, Price CJ. Voxel-based morphometry of herpes simplex encephalitis. Neuroimage 2001;13(4):623–631.
27. Bodini B, Khaleeli Z, Cercignani M, Miller DH, Thompson AJ, Ciccarelli O. Exploring the relationship between white matter and

gray matter damage in early primary progressive multiple sclerosis: an in vivo study with TBSS and VBM. Hum Brain Mapp 2009; 30(9):2852–2861.

28. Fjell AM, Westlye LT, Greve DN, et al. The relationship between diffusion tensor imaging and volumetry as measures of white matter properties. Neuroimage 2008;42(4): 1654–1668.

29. McDonald CR, Ahmadi ME, Hagler DJ, et al. Diffusion tensor imaging correlates of memory and language impairments in temporal lobe epilepsy. Neurology 2008;71(23): 1869–1876.

30. Nestor PG, Kubicki M, Kuroki N, et al. Episodic memory and neuroimaging of hippocampus and fornix in chronic schizophrenia. Psychiatry Res 2007;155(1):21–28.

31. Kelley WM, Miezin FM, McDermott KB, et al. Hemispheric specialization in human dorsal frontal cortex and medial temporal lobe for verbal and nonverbal memory encoding. Neuron 1998;20(5):927–936.

32. Golby AJ, Poldrack RA, Brewer JB, et al. Material-specific lateralization in the medial temporal lobe and prefrontal cortex during memory encoding. Brain 2001;124(pt 9): 1841–1854.

33. Dobbins IG, Kroll NE, Tulving E, Knight RT, Gazzaniga MS. Unilateral medial temporal lobe memory impairment: type deficit, function deficit, or both? Neuropsychologia 1998;36(2):115–127.

34. Glikmann-Johnston Y, Saling MM, Chen J, Cooper KA, Beare RJ, Reutens DC. Structural and functional correlates of unilateral mesial temporal lobe spatial memory impairment. Brain 2008;131(pt 11):3006–3018.

35. Hjalmarsson A, Blomqvist P, Sköldenberg B. Herpes simplex encephalitis in Sweden, 1990-2001: incidence, morbidity, and mortality. Clin Infect Dis 2007;45(7):875–880.